Physical Origin of the Optical Degradation of InAs Quantum Dot Lasers

Matteo Buffolo, Fabio Samparisi, Carlo De Santi, Daehwan Jung, *Member, IEEE*, Justin Norman, *Member, IEEE*, John E. Bowers, *Fellow, IEEE*, Robert W. Herrick, *Senior Member, IEEE*, Gaudenzio Meneghesso, *Fellow, IEEE*, Enrico Zanoni, *Fellow, IEEE*, and Matteo Meneghini, *Senior Member, IEEE*

***Abstract*— We present an extensive analysis of the physical mechanisms responsible for the degradation of 1.3-μm InAs quantum dot lasers epitaxially grown on Si, for application in silicon photonics. For the first time, we characterize the degradation of the devices by combined electro-optical measurements, electroluminescence spectra, and current-voltage analysis. We demonstrate the following original results: when submitted to a current step-stress experiment: 1) QD lasers show a measurable increase in threshold current, which is correlated to a decrease in slope efficiency; 2) the degradation process is stronger, when devices are stressed at current higher than 200 mA, i.e., in the stress regime, where both ground-state and excited-state emission are present; and 3) in the same range of stress currents, an increase in the defect-related current components is also detected, along with a slight decrease in the series resistance. Based on the experimental evidence collected within this paper, the degradation of QD lasers is ascribed to a recombination-enhanced defect reaction (REDR) process, activated by the escape of electrons out of the quantum dots.**

***Index Terms*— Quantum dots, lasers, degradation, semiconductor defects, carrier escape, reliability.**

I. Introduction

THE need for on-chip emitters on silicon is rapidly increasing, driven by the need for photonic integrated circuits for data communications and telecommunications, and sensors such as LIDARs and gyroscopes. For use in data communications, laser diodes need to have a high efficiency and a low cost, and must be monolithically integrated in large-scale silicon systems. Laser diodes are typically integrated on a silicon platform by means of wafer bonding [1]. As an alternative, III-V lasers can be epitaxially grown on a silicon substrate: this could increase the yield and scale of integration, thus reducing the cost of the manufacturing process. However, the direct epitaxial growth of III-V lasers on silicon is complicated by the large lattice mismatch that results in high dislocation densities [2], [3]. The performance of quantum-well laser diodes epitaxially grown on silicon is limited by the high defectiveness of the semiconductor material and lifetimes are limited to a few hundred hour [2], [4], [5]. For this reason, a significant research effort has been done to the study of III-V quantum-dot (QD) laser diodes, grown on a silicon substrate (see for instance [6], [7]). These devices are less affected by defect-related non-radiative recombination, compared to quantum well devices, thanks to the localization of carriers within the dots, which limits Shockley-Read-Hall (SRH) effects at dislocations. Compared to QW lasers, QD emitters have also a lower threshold current density [8], thus permitting a significant optimization of the energy efficiency.

In order to find application in silicon photonics, laser diodes must show a stable threshold current over time; for this reason, the reliability of QD lasers is currently under investigation. Pioneering reports have been published in the literature, and can be summarized as follows: 1) the first study on the reliability of InAs/GaAs quantum dot lasers grown on silicon, published in 2015 [9], demonstrated an extrapolated mean time to failure of 4600 h, and indicated that degradation may be related with the slow growth of dislocations; 2) a more recent study demonstrated an extrapolated lifetime of over 100158 h under moderate stress conditions (1.75 times the initial threshold current) [10]; 3) degradation rate is strongly dependent on the threading dislocation density (TDD); by reducing TDD from 2.8×10^8 cm^{-2} to 7.3×10^6 cm^{-2}, lifetime can be improved by five orders of magnitude, with reference to continuous-wave stress at 35° C [11]

The aim of this paper is to contribute to the understanding of the physical origin of the degradation of QD lasers epitaxially grown on a silicon substrate. For the first time, we have used several experimental techniques to investigate the physical mechanisms responsible for the degradation process, including

Manuscript received January 23, 2019; revised March 29, 2019; accepted April 2, 2019. Date of publication April 9, 2019; date of current version April 18, 2019. This work was supported in part by the INTERNET OF THINGS: SVILUPPI METODOLOGICI, TECNOLOGICI E APPLICATIVI project, co-founded (2018–2022) by the Italian Ministry of Education, Universities and Research (MIUR) under the aegis of the "Fondo per il finanziamento dei dipartimenti universitari di eccellenza" initiative (Law 232/2016), and in part by the U.S. Department of Energy Advanced Research Project Agency under Grant DE-AR000067. *(Corresponding author: Matteo Buffolo.)*

M. Buffolo, F. Samparisi, G. Meneghesso, E. Zanoni, and M. Meneghini are with the Department of Information Engineering, University of Padova, 35131 Padova, Italy (e-mail: matteo.buffolo@dei.unipd.it; fabio.samparisi@phd.unipd.it; gauss@dei.unipd.it; zanoni@dei.unipd.it; matteo.meneghini@dei.unipd.it).

C. De Santi is with the Department of Information Engineering, University of Padova, 35131 Padova, Italy, and also with the Centro Giorgio Levi Cases, University of Padova, 35131 Padova, Italy (e-mail: carlo.desanti@dei.unipd.it).

D. Jung is with the Center for Opto-Electronic Materials and Devices, Korea Institute of Science and Technology, Seoul 02792, South Korea (e-mail: daehwan.jung.ucsb@gmail.com).

J. Norman and J. E. Bowers are with the Department of Electrical and Computer Engineering, University of California, Santa Barbara, CA 93106 USA (e-mail: jcnorman223@gmail.com; bowers@ece.ucsb.edu).

R. W. Herrick is with Intel Corporation, Santa Clara, CA USA (e-mail: robert.w.herrick@intel.com).

Color versions of one or more of the figures in this paper are available online at http://ieeexplore.ieee.org.

Digital Object Identifier 10.1109/JQE.2019.2909963

current-voltage characterization, spectrally-resolved electroluminescence and L-I characterization. The results collected within this paper indicate that: (i) the analyzed QD lasers can operate in two regimes. For I<200 mA, only ground-state (GS) emission is observed, while for higher current levels the emission from the excited state (ES) starts dominating; (ii) current stress induces an increase in the threshold current, well correlated to a decrease in slope efficiency; (iii) degradation rate is stronger for stress currents higher than 200 mA, i.e. when emission from ES and carrier escape are dominant; finally, (iv) the current-voltage characterization revealed that stress induced an increase in the defect-related current components, and a moderate decrease in series resistance. The degradation is ascribed to the escape of carriers out of the quantum dots, with consequent recombination at non-radiative defects and recombination-enhanced defect reaction (REDR). Such effect is more prominent when the devices are stressed at I>200 mA, since a high escape rate is reached when the carriers populate the excited state.

II. Experimental Details

The study was carried out on quantum-dot laser diodes grown by solid-source MBE on on-axis (001) GaP/Si substrates. In particular, a 45 nm thick pseudomorphic GaP buffer layer was grown on the Si substrate; then, the structure consists of a 3100 nm n-type GaAs buffer, a 1500 nm n-AlGaAs cladding, a 50 nm unintentionally doped (uid)-GaAs waveguide, a 3× sequence of InAs QDs in InGaAs QWs and related barrier, a uid-GaAs waveguide, a 1510 nm p-AlGaAs cladding and a 300 nm p-GaAs contact layer. The GaAs barriers were p-doped at 5×10^{17} cm^{-3} using Be, corresponding to $\sim$ 10 holes per QD. A threading dislocation density of about 7×10^6 cm^{-2} was achieved in proximity of the active region.

The material was processed into ridge-waveguide lasers, and the devices were cleaved after thinning of the silicon substrate to 150 μm. Cavity width and length are 3 μm and 1000 μm respectively, corresponding to a device area of 3000 μm^2. Average threshold current at 25° C is 17 mA, corresponding to 567 A/cm^2, whereas the maximum output power is $\approx$ 34 mW, at 20° C and I = 230 mA Additional details on the growth and on the epitaxial structure of the devices can be found in [12]

The devices were submitted to a current step-stress experiment; stress current was increased by 10 mA every hour, starting from 10 mA. The stress experiment was interrupted at 300 mA, i.e. when a significant degradation of the device performance was reached. After each stage of the step-stress experiment, a full characterization of device performance was carried out. For the stress experiment, the samples were never moved from their position. LDs were mounted on a Peltier-controlled baseplate; a bifurcated optical fiber bundle was used to simultaneously read the optical power through a photodiode and the electroluminescence spectra through an optical spectrum analyzer. High resolution (pA-range) current-voltage characteristics were also measured with the aim of evaluating changes in the defect-related current components.

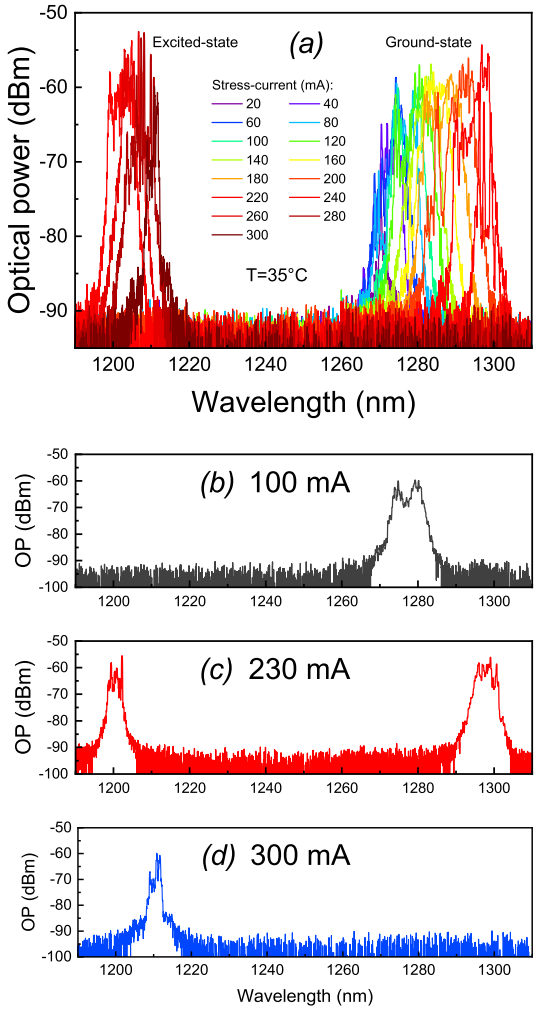

Fig. 1. (a) EL spectra collected at increasing current during the execution of the step-stress experiment at T_{AMB} = 35° C; (b), (c), (d) EL spectra collected at three different current levels, corresponding to ground-state only, both ground-state and excited-state, excited-state only. The emission from the wetting layer, expected to be within the 900 nm - 1000 nm range [13], was not observed.

III. Results

A. Spectral Analysis as a Function of Current

A first step for understanding the degradation data described in this paper is the evaluation of the dominant emission processes taking place during the step-stress experiment. To this aim, we carried out electroluminescence measurements at increasing stress currents, from 20 mA to 300 mA, at a baseplate temperature (T_{AMB}) of 35° C. The results of this analysis are summarized in Figure 1, that reports (a) the EL spectra collected during stress at all investigated current levels, and (b), (c), (d) the EL spectra collected at 100 mA, 230 mA, 300 mA. All spectra have been smoothed in order to remove fringes related to cavity modes and improve readability. As can be noticed (Figure 1 (a)), at 20 mA the EL spectrum is centered around 1270 nm; with increasing current, a red-shift of peak wavelength is observed. This is ascribed to self-heating and the consequent bandgap narrowing, considering that the EL spectra were collected in dc conditions, with integration time of 20 s to ensure high sensitivity in the whole

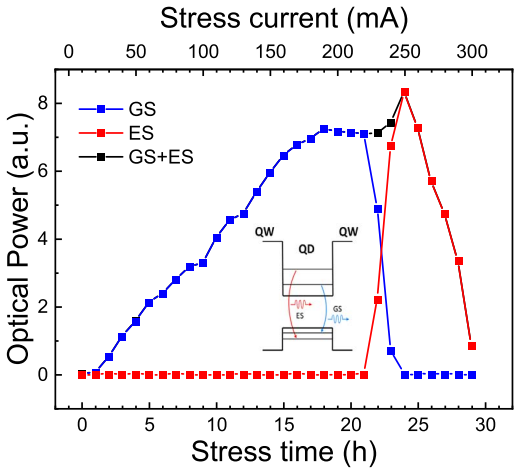

Fig. 2. Variation of the luminescence from the ground (GS) and excited (ES) state with increasing stress current. Total integrated optical power (GS+ES) is also plotted for comparison. Inset figure shows a simplified band-diagram of the Dots-In-Well (DWELL) region indicating the transitions related to GS and ES emissions (wetting layer omitted).

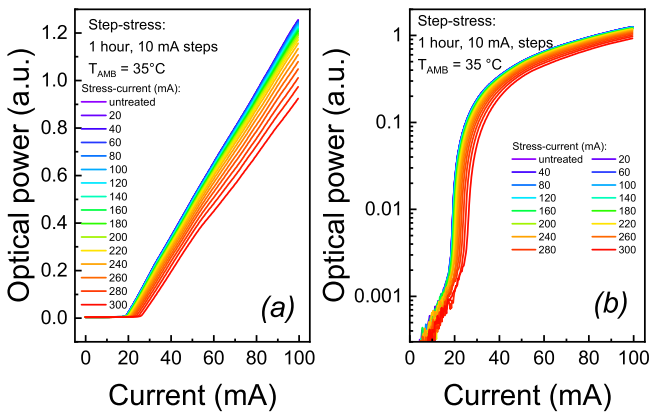

Fig. 3. L-I curves measured at different stages of the stepstress experiment, plotted in (a) linear and (b) semi-logarithmic scale.

analyzed current range. For currents lower than 200 mA, only one spectral peak is observed, related to the emission from the ground-state (GS) of the quantum-dots (Figure 1 (b)). At higher currents (210-240 mA), a second peak centered around 1200 nm is observed. This emission is ascribed to the recombination from the excited state (ES) of the quantum dots (Figure 1 (c)). At higher currents (between 250 mA and 300 mA), only emission from the ES is observed, while GS signal is completely quenched (Figure 1 (d)).

A better description of the interplay between ground and excited states is given by Figure 2, showing the integral of GS and ES emission, along with the total integrated emission (ES+GS). GS emission increases monotonically with current, starting from 20 mA up to 190 mA. For currents between 190 mA and 230 mA, total (GS+ES) emission shows a plateau: emission from GS saturates, and carriers start being transferred to the ES. The excited state starts lasing above 210 mA (see also the spectra in Figure 1 (a)), and beyond this point GS emission starts decreasing. Between 230 mA and 250 mA integrated EL further increases slightly, while for currents higher than 250 mA also emission from ES quenches completely. Almost no emission is observed at 300 mA, indicating that a considerable amount of injected carriers is lost non-radiatively.

To explain the results in Figure 1 and Figure 2, we refer to the data and numerical simulations discussed in [14], [15]: the hypothesis is that GS and ES have two different threshold current levels (I_{th_GS}, I_{th_ES}), with $I_{th_ES} > I_{th_GS}$. When GS lasing is reached, the carrier density at GS will be clamped; for current levels between I_{th_ES} and I_{th_GS}, carriers can start filling the ES. The hole occupation of GS and ES are linked, due to the low energy separation of the two states for holes [14]. On the other hand, the density of electrons in the excited state will increase with increasing current. Two state lasing (Figure 1) becomes possible for $I > I_{th_GS}$, since ES occupation increases while GS inversion remains clamped at the threshold level of GS.

The quenching of ground-state emission for $I > I_{th_GS}$ can be explained by three possible processes (see [15] and references therein): (i) at high currents, self-heating becomes prevalent. Based on occupation probability, normally ES is less occupied than GS. This difference is supposed to disappear at high temperature levels, and ES will start lasing. When ES and GS have comparable level of occupation, ES will be the only one lasing, due to its higher degeneracy [15], [16]. This mechanism is compatible with the strong self-heating progressively experienced by the sample in high-current regime, testified by the considerable redshift of the EL spectra with increasing stress current (Fig. 1a).(ii) A second explanation considers a current-dependent homogeneous broadening, with consequent decrease in the maximum gain [17]. (iii) Finally, the competition for holes between GS and ES has been considered. At high current levels, if hole injection is not sufficient, ES emission will consume all the available holes, due to its higher degeneracy, thus leading to a quenching of GS [18]. It has already been demonstrated that due to the non-negligible SRH recombination in proximity of the active layers of the device, a limited supply of holes to the quantum dots has a strong negative impact on both optical efficiency and reliability [11]. While this problem was partially circumvented by employing a modulation p-doping approach, which increases the capture rate of holes from the QDs, this behavior shows that for this kind of devices the reduced hole injection represents a limiting factor, further supporting the role of this process in the balance between GS and ES emissions. Finally, at very high current levels (I∼300 mA), escape and overflow processes become dominant. As a consequence, carriers will not be captured efficiently by the quantum dots, and escape towards the wells will dominate. Hence, population inversion will no longer be reached, and also ES will stop lasing.

B. Impact of Stress on the Optical Characteristics

The L-I curves of the laser diode during stress at increasing current are shown in Figure 3. As can be noticed, stress induced an increase in the threshold current of the devices, and a decrease in the slope efficiency. A better description of the degradation kinetics is given by Figure 4, that reports the I_{th} increase and SE decrease as a function of stress time/current. Two phases can be clearly identified: when stress

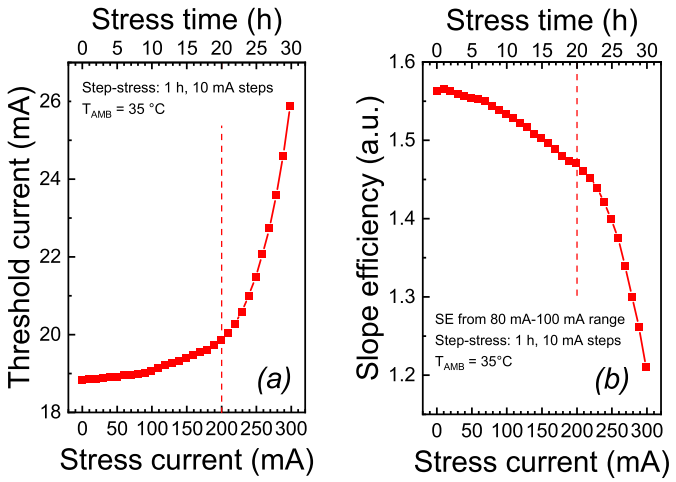

Fig. 4. (a) Threshold current and (b) slope efficiency variation during the step-stress experiment. A significant change in both parameters is observed for stress currents higher than 200 mA.

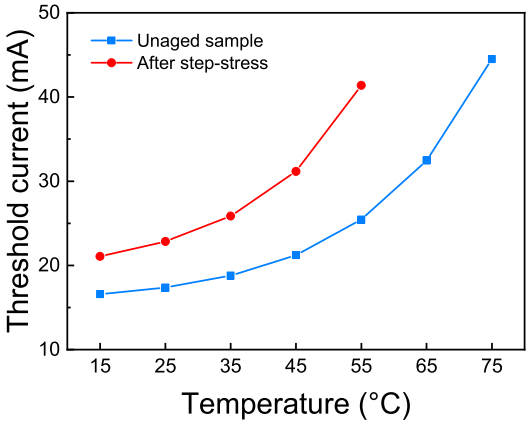

Fig. 5. Threshold current as a function of baseplate temperature (TAMB) measured before and after the step-stress experiment. After stress, no lasing was observed within the bias and temperature range employed for the optical characterization.

current is low/moderate (I<200 mA), the threshold current increases slowly, from 18.8 mA (before stress) to 19.6 mA (after the step at 200 mA). In the same time frame, also slope efficiency decreases gradually from 100 % to 96.3 % of the original value observed on the unaged laser. On the other hand, for higher stress currents (up to 300 mA), a significant increase in the degradation rate is observed. Threshold current increases from 20 mA to 26 mA when current is increased from 200 mA to 300 mA, while slope efficiency shows also a quick variation from 96.3 % to 83.9 %. Figure 3 also shows that the decrease in the slope efficiency of the devices is stronger at high measuring current levels (I>70 mA), compared with what happens in the low current regime.

Figure 5 shows the variations in the threshold current-temperature curves induced by the step-stress. In particular, the plot shows that while stress induced a general increase in threshold current across the entire range of measuring temperature employed, a stronger variation is observed for higher measuring temperatures. This decreased optical efficiency at higher temperatures can either be attributed to an

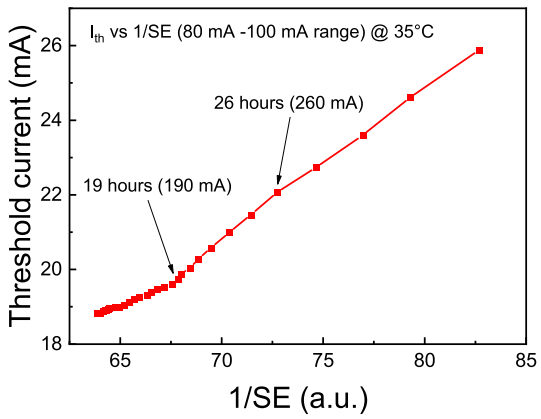

Fig. 6. Relation between the variation in threshold current (I_{th}) and the change in the reciprocal of slope efficiency (1/SE).

increase in the SRH recombination, due the increase in defect concentration within the active region, or to the increase in the carrier escape rate from the active volume of the quantum dots. Interestingly, within the temperature range under investigation, the I_{th}-T relation was not showing a purely exponential trend. This is in agreement with previous reports showing that both IR QW-based LDs [19]–[21] and DWELL 1.3 μm lasers [22] exhibit around RT a change in the temperature dependence of threshold current, due to the increased carrier leakage from the active region. This process lowers the characteristic temperature T_0 of the laser at high measuring temperatures, thus lowering the optical performance of the device.

To achieve a better understanding of the degradation process, we evaluated the link between the degradation of threshold current and slope efficiency.

The results (Figure 6) indicate that the variation in threshold current is linearly correlated to the change in 1/SE, i.e. the reciprocal of slope efficiency. Based on laser theory, we know that slope (or differential) efficiency can be expressed as:

$$SE = \eta_i \frac{\alpha_m}{\alpha_m + \alpha_i} \tag{1}$$

where η_i, called injection efficiency, represents the fraction of the terminal current that generates carriers in the active region, while α_i and α_m are the internal and mirror losses. On the other hand, threshold current can be calculated by evaluating the below-threshold rate equation for threshold carrier density N_{TH}, ad by assuming that the injection efficiencies in LED mode and above-threshold are equal [23],

$$\frac{\eta_i I_{TH}}{qV} = \left(R_{SRH} + R_{sp} + R_{\text{Auger}}\right) = \frac{N_{TH}}{\tau} \tag{2}$$

Indicating that threshold current is inversely proportional to the injection efficiency, as follows:

$$I_{TH} \cong \frac{qVN_{TH}}{\eta_i \tau} \tag{3}$$

Here R_{SRH}, R_{sp}, R_{Auger} are the Shockley-Read-Hall, spontaneous and Auger recombination rates, q is the electron charge, N_{th} is the threshold carrier density, τ is the electron lifetime and V is the volume of the active region. The results in Figure 6 (i.e. the linear relation between the variations of I_{th} and SE) can be explained by considering

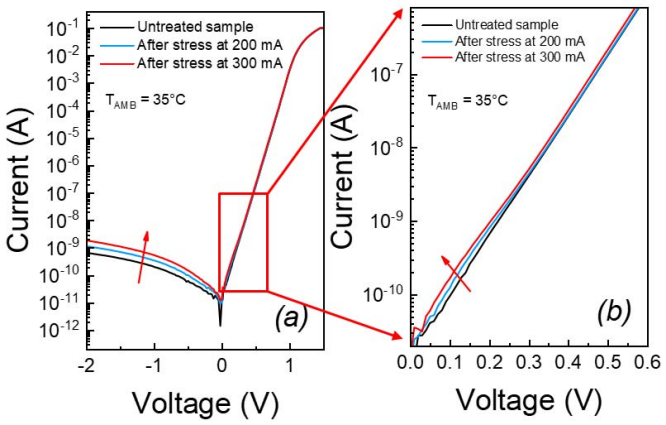

Fig. 7. I-V plots collected before stress, after stress at 200 mA, after stress at 300 mA (intermediate steps are not shown for clarity). Stress induced an increase in the reverse current and in the sub-threshold forward-leakage.

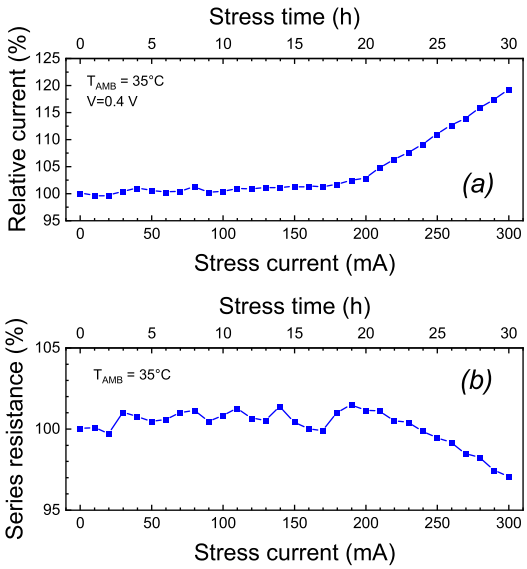

Fig. 8. Variation in (a) sub-threshold forward leakage and (b) series resistance during the step-stress experiment.

Equations (1) and (3), and are consistent with the hypothesis that stress induced a change in injection efficiency, which is directly proportional to SE and inversely proportional to I_{th}. Based on this assumption, we suggest that stress is inducing a decrease in the fraction of carriers captured by the quantum dot or, equivalently, an increase in the escape rate.

C. Changes in the Electrical Parameters and Discussion

The electrical parameters of the devices were evaluated by means of current-voltage characterization. Figure 7 reports the I-V curves collected during one step-stress experiment: as can be noticed, the I-V plots showed a generally stable behavior during stress up to 300 mA. However, small, but meaningful, changes were detected: stress was found to induce an increase in the reverse leakage current. At the same time (Figure 7 (b)), an increase in the low-forward bias current was observed. In both regimes (reverse and low-forward), current originates from defect-related conduction [24]–[26]. Hopping through traps can favor reverse leakage [27], while trap-assisted tunneling can contribute to forward-conduction [28].

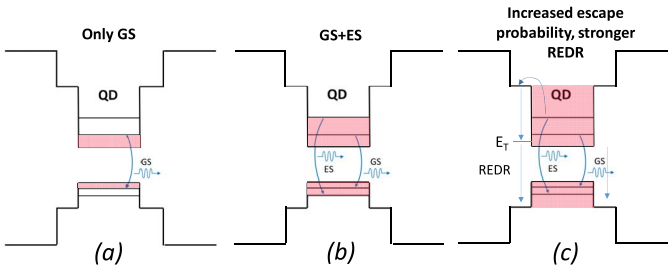

Fig. 9. Schematic model to explain the degradation process induced by the presence of the excited state, and related to the escape of carriers and subsequent recombination in the QWs through deep levels.

Figure 8 (a) provides more insight on the time-dependence of the degradation process: as can be noticed, defect-related forward leakage showed the strongest increase for stress currents higher than 200 mA. Also, minor variations in series resistance were observed (4 % decrease after the stress at 300 mA). The results in Figure 7 and Figure 8 (a) suggest that stress induced the generation of defects within the active region of the devices.

D. Model for the Degradation Process

The results described above can be summarized as follows:

a. Stress induces an increase in threshold current, correlated with a decrease in slope efficiency; the correlation between the variation of the two parameters suggests that stress induces a decrease in injection efficiency, either due to the loss of carriers caused by recombination through defects in proximity of the QD layers, or to the increase in the carrier escape rate;
b. The degradation rate is higher for stress currents higher than 200 mA, i.e. in the current regime where – according to the spectral measurements – emission from the excited state dominates;
c. The results of the electrical characterization support the hypothesis that stress induced the generation of defects within the active region of the devices.

We propose to explain the observed degradation data as follows (see the schematic drawing in Figure 9): at low stress currents (up to 190 mA), only ground state is populated, carriers are effectively confined in the quantum dots, and excess electrons recombine through stimulated emission at 1270 nm (nominal wavelength of the devices, Figure 9 (a)). Thanks to the strong confinement of the quantum dots, carriers can not reach dislocation-related defects, and this prevents SRH recombination and defect reactions [9]. For higher stress current (between 190 mA and 230 mA), two-state emission becomes possible (Figure 9 (b)), and carriers start populating the excited state. Finally, for currents higher than 230 mA, lasing occurs only at the excited mode, until a full quenching of electroluminescence is reached, once current gets close to 300 mA (Figure 9 (c)).

In the last two conditions ((Figure 9 (b) and (c)), carrier escape out of the quantum dots starts becoming relevant. In the same current range, a high degradation rate is observed. Based

on these considerations, we ascribe degradation to the escape of carriers out of the quantum dots: once electrons/holes escape, they can reach and overcome the wetting layer and migrate to the quantum wells, thus no longer being spatially confined. As a consequence, carriers can move laterally, thus reaching extended defects/dislocations present within the active layers of the device (Figure 9 (c)).

Non-radiative recombination of carriers at highly-defective sites can promote the generation/propagation of dislocations and dislocation-related defects, and a consequent increase in SRH losses and threshold current. In this view, degradation would proceed through recombination-enhanced defect reaction (REDR). The propagation of defects also reduces the capture rate from QDs, either by changing the electrostatic potential in proximity of active region (due to the generation of charge defects), or by reducing the effective concentration of non-degraded quantum dots contributing to the stimulated emission process. This eventually reduces the injection efficiency and leads to the decrease in slope efficiency. This interpretation is consistent with recent reports [11] demonstrating that dislocations play a key role in the degradation process: a reduction in the density of extended defects can significantly reduce the degradation rate, thanks to the reduction in REDR phenomena.

IV. Conclusion

In summary, we have presented an extensive investigation of the physical origin of degradation of InAs quantum-dot lasers submitted to step-stress experiment. For the first time, we have used spectral measurements, optical analysis and electrical characterization to describe the physics of degradation. The results collected suggest that carrier escape plays a strong role in favoring device degradation. When the devices are stressed at low current densities, carriers are confined by the quantum dots and can not diffuse laterally, thus being prevented from reaching defects located within the quantum wells or the wetting layer. On the other hand, at high stress currents carriers can first recombine on the excited state, then escape out of the quantum dots, thus recombining non-radiatively at dislocations. This can promote recombination-enhanced defect reactions, leading to the generation of lattice defects. As a consequence, both threshold current increase and a worsening in injection efficiency are observed.

Acknowledgments

The authors would like to thank Kunal Mukherjee and Jennifer Selvidge for useful conversations.

References

[1] K. Tanabe, T. Rae, K. Watanabe, and Y. Arakawa, "High-temperature 1.3 μm InAs/GaAs quantum dot lasers on Si substrates fabricated by wafer bonding," *Appl. Phys. Express*, vol. 6, no. 8, 2013, Art. no. 082703.

[2] A. Y. Liu *et al.*, "High performance continuous wave 1.3 μm quantum dot lasers on silicon," *Appl. Phys. Lett.*, vol. 104, no. 4, Jan. 2014, Art. no. 041104.

[3] Y.-G. Zhou, C. Zhou, C.-F. Cao, J.-B. Du, Q. Gong, and C. Wang, "Relative intensity noise of InAs quantum dot lasers epitaxially grown on Ge," *Opt. Express*, vol. 25, no. 23, pp. 28817–28824, Nov. 2017.

[4] H. Kroemer, T.-Y. Liu, and P. M. Petroff, "GaAs on Si and related systems: Problems and prospects," *J. Cryst. Growth*, vol. 95, nos. 1–4, pp. 96–102, Feb. 1989.

[5] K. Morizane, "Antiphase domain structures in GaP and GaAs epitaxial layers grown on Si and Ge," *J. Cryst. Growth*, vol. 38, no. 2, pp. 249–254, May 1977.

[6] T. Wang, H. Liu, A. Lee, F. Pozzi, and A. Seeds, "1.3-μm InAs/GaAs quantum-dot lasers monolithically grown on Si substrates," *Opt. Express*, vol. 19, no. 12, pp. 11381–11386, Jun. 2011.

[7] D. Jung *et al.*, "Highly reliable low-threshold InAs quantum dot lasers on on-axis (001) Si with 87% injection efficiency," *ACS Photon.*, vol. 5, no. 3, pp. 1094–1100, Mar. 2018.

[8] D. G. Deppe, K. Shavritranuruk, G. Ozgur, H. Chen, and S. Freisem, "Quantum dot laser diode with low threshold and low internal loss," *Electron. Lett.*, vol. 45, no. 1, pp. 54–56, 2009.

[9] A. Y. Liu, R. W. Herrick, O. Ueda, P. M. Petroff, A. C. Gossard, and J. E. Bowers, "Reliability of InAs/GaAs quantum dot lasers epitaxially grown on silicon," *IEEE J. Sel. Topics Quantum Electron.*, vol. 21, no. 6, pp. 690–697, Nov. 2015.

[10] S. Chen *et al.*, "Electrically pumped continuous-wave III–V quantum dot lasers on silicon," *Nature Photon.*, vol. 10, no. 5, pp. 307–311, May 2016.

[11] D. Jung *et al.*, "Impact of threading dislocation density on the lifetime of InAs quantum dot lasers on Si," *Appl. Phys. Lett.*, vol. 112, no. 15, Apr. 2018, Art. no. 153507.

[12] D. Jung *et al.*, "High efficiency low threshold current 1.3 μm InAs quantum dot lasers on on-axis (001) GaP/Si," *Appl. Phys. Lett.*, vol. 111, no. 12, Sep. 2017, Art. no. 122107.

[13] A. Y. Liu *et al.*, "MBE growth of P-doped 1.3 μm InAs quantum dot lasers on silicon," *J. Vac. Sci. Technol. B, Microelectron.*, vol. 32, no. 2, Mar. 2014, Art. no. 02C108.

[14] A. Röhm, B. Lingnau, and K. Lüdge, "Understanding ground-state quenching in quantum-dot lasers," *IEEE J. Quantum Electron.*, vol. 51, no. 1, pp. 1–11, Jan. 2015.

[15] A. Röhm, K. Lüdge, and E. Schöll, *Dynamic Scenarios in Two-State Quantum Dot Lasers: Excited State Lasing, Ground State Quenching, and Dual-Mode Operation*. Wiesbaden, Germany: Springer Fachmedien Wiesbaden, 2015.

[16] K. Lüdge and E. Schöll, "Temperature dependent two-state lasing in quantum dot lasers," in *Proc. 5th Rio De La Plata Workshop Laser Dyn. Nonlinear Photon.*, Dec. 2011, pp. 1–6.

[17] M. Sugawara *et al.*, "Modeling room-temperature lasing spectra of 1.3-μm self-assembled InAs/GaAs quantum-dot lasers: Homogeneous broadening of optical gain under current injection," *J. Appl. Phys.*, vol. 97, no. 4, Feb. 2005, Art. no. 043523.

[18] E. A. Viktorov, P. Mandel, Y. Tanguy, J. Houlihan, and G. Huyet, "Electron-hole asymmetry and two-state lasing in quantum dot lasers," *Appl. Phys. Lett.*, vol. 87, no. 5, Aug. 2005, Art. no. 053113.

[19] S. Seki, H. Oohashi, H. Sugiura, T. Hirono, and K. Yokoyama, "Study on the dominant mechanisms for the temperature sensitivity of threshold current in 1.3-μm InP-based strained-layer quantum-well lasers," *IEEE J. Quantum Electron.*, vol. 32, no. 8, pp. 1478–1486, Aug. 1996.

[20] A. F. Phillips, S. J. Sweeney, A. R. Adams, and P. J. A. Thijs, "The temperature dependence of 1.3- and 1.5-μm compressively strained InGaAs(P) MQW semiconductor lasers," *IEEE J. Sel. Top. Quantum Electron.*, vol. 5, no. 3, pp. 401–412, May/Jun. 1999.

[21] M. Ishikawa, H. Shiozawa, K. Itaya, G. Hatakoshi, and Y. Uematsu, "Temperature dependence of the threshold current for InGaAlP visible laser diodes," *IEEE J. Quantum Electron.*, vol. 27, no. 1, pp. 23–29, Jan. 1991.

[22] L. V. Asryan and R. A. Suris, "Characteristic temperature of quantum dot laser," *Electron. Lett.*, vol. 33, no. 22, pp. 1871–1872, Oct. 1997.

[23] P. M. Smowton and P. Blood, "The differential efficiency of quantum-well lasers," *IEEE J. Sel. Topics Quantum Electron.*, vol. 3, no. 2, pp. 491–498, Apr. 1997.

[24] N. F. Hasbullah, J. P. R. David, and D. J. Mowbray, "Dark current mechanisms in quantum dot laser structures," *J. Appl. Phys.*, vol. 109, no. 11, Jun. 2011, Art. no. 113111.

[25] P. R. Griffin *et al.*, "Effect of strain relaxation on forward bias dark currents in GaAs/InGaAs multiquantum well *p–i–n* diodes," *J. Appl. Phys.*, vol. 80, no. 10, p. 5815, Aug. 1998.

[26] A. M. Sanchez, R. Beanland, N. F. Hasbullah, M. Hopkinson, and J. P. R. David, "Correlation between defect density and current leakage in InAs/GaAs quantum dot-in-well structures," *J. Appl. Phys.*, vol. 106, no. 2, Jul. 2009, Art. no. 024502.

[27] Q. Shan *et al.*, "Transport-mechanism analysis of the reverse leakage current in GaInN light-emitting diodes," *Appl. Phys. Lett.*, vol. 99, no. 25, 2011, Art. no. 253506.

[28] M. Mandurrino *et al.*, "Physics-based modeling and experimental implications of trap-assisted tunneling in InGaN/GaN light-emitting diodes," *Phys. Status Solidi*, vol. 212, no. 5, pp. 947–953, May 2015.

Matteo Buffolo was born in Vittorio Veneto, Italy, in 1986. He received the master's degree in electronic engineering from the University of Padua, in 2014, with a thesis focusing on the analysis of the degradation mechanisms of GaN-based mid-power white LEDs, and the Ph.D. degree from the Department of Information Engineering, University of Padua. He holds a post-doctoral position at the University of Padua. His research interests include the reliability of lighting systems employing GaN-based devices (lasers and LEDs) and the investigation of the degradation mechanisms that affect modern IR laser sources for integrated telecommunication applications.

Fabio Samparisi was born in Vienna, Austria, in 1992. He received the master's degree in electronic engineering from the University of Padua, in 2018, with a master's thesis on reliability and the degradation mechanisms of InAs quantum-dot lasers for silicon photonics applications. He is currently pursuing the Ph.D. degree with the Department of Information Engineering, University of Padua, where he is involved in the design and realization of instrumentation for ultrafast optics in the XUV and soft X-ray spectral region.

Carlo De Santi was born in Verona, Italy, in 1985. He received the Ph.D. degree in 2014. He holds a post-doctoral position at the Microelectronics Group, University of Padua. His main research activities are characterization, physical modeling, and the reliability of various GaN-, GaAs-, InP-, Ga_2O_3-, CdTe-, and Si-based electronic and optoelectronic devices. He has authored over 30 peer-reviewed journal papers, 50 contributions in conference proceedings, and four book chapters.

Daehwan Jung (M'16) received the Ph.D. degree in electrical engineering from Yale University in 2016. He was a Post-Doctoral Researcher with the University of California at Santa Barbara for two years. In 2019, he started working at the Korea Institute of Science and Technology as a Senior Research Scientist. His research interest is to study novel III–V materials growth for high-performance optoelectronic devices.

Justin Norman (M'14) received the B.S. degree in chemical engineering and physics from the University of Arkansas at Fayetteville, Fayetteville, AR, USA, in 2013, and the Ph.D. degree in materials from the University of California at Santa Barbara, CA, USA, in 2018, as a National Science Foundation Graduate Research Fellow and a Frenkel Foundation Fellow. He is currently a Post-Doctoral Researcher with the University of California at Santa Barbara. He is currently involved in the heteroepitaxy of III–V materials on Si for photonic integration. His research interest is in the growth of InAs quantum dots via molecular beam epitaxy for applications in photonics and quantum electrodynamics.

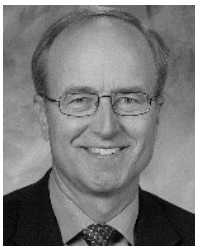

John E. Bowers (F'–) is the Director of the Institute for Energy Efficiency. He is a member of the National Academy of Engineering and the National Academy of Inventors. He is a fellow of the OSA and the American Physical Society. He was a recipient of the IEEE Photonics Award, the OSA Tyndall Award, the OSA Holonyak Prize, and the IEEE LEOS William Streifer Award. He is the Fred Kavli Chair of nanotechnology.

Robert W. Herrick (S'81–M'87–SM'05) received the M.S.E.E. from the University of Illinois in 1987. He was with McDonnell Douglas, where he was involved in early OEIC and high-power laser Research andDevelopment, device modeling, mask design, and process development. After gaining an interest in reliability physics from the late Dr. R. G. Waters, he went to UCSB, and he did the first studies in VCSEL degradation for the Ph.D. dissertation with Prof. L. Coldren and Prof. P. Petroff. In the past 20 years, he was specialized in semiconductor laser reliability and failure analysis, and he has written many the most-cited papers and invited book review chapters on the subject. He was a Laser Reliability Engineer for many large fiber-optics companies in Silicon Valley, including HP/Agilent, Emcore, Finisar, and JDSU/Lumentum. He is responsible for laser reliability at Intel's Silicon Photonic Product Division. He has been with Intel since 2013.

Gaudenzio Meneghesso (S'95–M'97–SM'07–F'13) received the degree in electronics engineering from the University of Padua in 1992, where was involved in failure mechanism induced by hot-electrons in MESFETs and HEMTs. Since 2011, he has been with the University of Padua, as a Full Professor. His research interests include electrical characterization, modeling, and the reliability of microelectronics devices. Within these activities, he has published over 800 technical papers (of which more than 100 invited papers and 12 best paper awards). He has been nominated as the IEEE Fellow class 2013, with the following citation: for contributions to the reliability physics of compound semiconductors devices.

Enrico Zanoni (S'81–A'82–SM'93–F'09) was born in Verona, Italy, in 1956. He received the Laurea degree *(cum laude)* in physics from the University of Modena and Reggio Emilia, Modena, Italy, in 1982. He has been a Full Professor of digital electronics with the Department of Information Engineering, University of Padua, Padua, Italy, since 1997.

Matteo Meneghini (S'06–M'08–SM'13) received the Ph.D. degree from the University of Padua, Padua, Italy, in 2008. He is currently an Assistant Professor with the Department of Information Engineering, University of Padua, where he is involved in electro-optical characterization and the modeling of the performance and reliability of LEDs, lasers, HEMTs, and advanced solar cells.